water

MDPI

Article

Simulation of Rainfall-Runoff Process in a Catchment with a Check-Dam System Equipped with a Perforated Riser Principal Spillway on the Loess Plateau of China

Zeyu Zhang [1], Junrui Chai [1,2,*], Shuilong Yuan [1], Zhanbin Li [1,3] and Zengguang Xu [1]

[1] State Key Laboratory of Eco-hydraulics in Northwest Arid Region of China, Xi'an University of Technology, Xi'an 710048, China; zzy_pap@163.com (Z.Z.); yuanshuilong@163.com (S.Y.); zhanbinli@126.com (Z.L.); xuzengguang@xaut.edu.cn (Z.X.)
[2] School of Civil Engineering, Xijing University, Xi'an 710123, China
[3] State Key Laboratory of Soil Erosion and Dry-land Farming on the Loess Plateau, Institute of Soil and Water Conservation, Chinese Academy of Sciences and Ministry of Water Resources, Yangling 712100, China
* Correspondence: jrchai@xaut.edu.cn

Abstract: Check dams are applied worldwide as an effective approach for soil and water conservation. To improve the simulation accuracy of the hydrological processes in a catchment with a check-dam system, this study analyzed the applicability and accuracy of a formula for the drainage process of a perforated riser principal spillway based on observational experiments. The rainfall-runoff processes in a catchment with a check-dam system were also simulated with the recommended formulas for the drainage process of a perforated riser principal spillway. The deviations in the calculated discharge from the observed values of the experiment with the recommended formulas under normal and abnormal working conditions were within ±15% and ±5%, respectively. The hydrologic model used in this study needed only a few parameters to achieve a satisfactory simulation accuracy. The recommended formulas for the drainage process of a perforated riser principal spillway can improve the simulation accuracy of a flood peak by 7.42% and 19.58% compared with the accuracies of the technical code formula scenario and no drainage scenario, respectively. The results of this study are expected to provide a reference for flood warnings and safe operations of check-dam systems.

Keywords: check dam; discharge structure; drainage process; hydrologic model

Citation: Zhang, Z.; Chai, J.; Yuan, S.; Li, Z.; Xu, Z. Simulation of Rainfall-Runoff Process in a Catchment with a Check-Dam System Equipped with a Perforated Riser Principal Spillway on the Loess Plateau of China. *Water* **2021**, *13*, 2450. https://doi.org/10.3390/w13172450

Academic Editor: Marco Franchini

Received: 14 June 2021
Accepted: 31 August 2021
Published: 06 September 2021

1. Introduction

A check dam is the most important soil and water conservation engineering measure on the Loess Plateau. Generally, a check dam is composed of a dam body and a drainage structure. Some simple check dams constructed in the early years consisted only of a dam body [1]. Check dams are widely constructed in channels to trap sediment [2], and with the increase in the number of check dams in a catchment, a completely functioning check-dam system forms gradually. Presently, there are 113,500 check dams over 5 m in height on the Loess Plateau [3,4]. Check dams are also widely used in other countries, such as Ethiopia [5], Spain [6,7], Iran [8], Italy [9], and Mexico [10].

Studies on check dams around the world have focused on their geomorphological and hydrological effects. Research methods have been gradually developed from field observation tests to physical-based hydrological and hydrodynamic models [11–14]. The distributed hydrological model Soil & Water Assessment Tool (SWAT) has been used by many researchers to simulate the hydrological and sediment processes of a catchment to analyze the reduction effect of check dams on runoff and sediment [1,15,16]. In SWAT, a check dam is regarded as a reservoir, only the discharge of the spillway can be taken into

account, and the drainage of a perforated riser principal spillway cannot be simulated [15,17]. Considering that the discharge capacity of a perforated riser principal spillway is relatively small, it is rational to ignore the drainage of a perforated riser principal spillway in the simulation of the hydrological processes of large watersheds, but it is inappropriate to ignore it in small catchments. Tang, et al. [18] simulated the effect of a check-dam system on hydrological processes with a distributed physical-based hydrological model (InHM), but the drainage of the perforated riser principal spillway was not simulated in the model. Wang, et al. [19] quantitively evaluated the effect of a check-dam system on catchment flood characteristics, and the drainage of the perforated riser principal spillway was simplified with the modification of topography to set a breach on the dam body. Yuan, et al. [14] coupled the distributed hydrological model MIKE SHE and the one-dimensional hydrodynamic model MIKE 11 to simulate the hydrological process of a catchment with a check-dam system, and the drainage of the perforated riser principal spillway was described by inputting the depth-discharge curve of the perforated riser principal spillway in the control structures module of MIKE 11; the results of the simulation were satisfactory. Hence, it is of great significance to take the drainage process of the perforated riser principal spillway into account in the simulation for the complete description of the hydrological process of a catchment with a check-dam system.

Since the drainage process of a perforated riser principal spillway should be added to the hydrological model, the applicability and accuracy of the formula for the drainage process of a perforated riser principal spillway are crucial for improving simulation efficiency. In fact, although the history of the utilizing and investigating perforated riser principal spillways is long [20–22], the majority of the investigations focused on risers perforated with circular orifices [23–25]. However, for the check dam, one of whose primary discharge structure types is the perforated riser principal spillway, the riser is often made from bricks, resulting in the application of rectangular orifices being more common than that of circular orifices. In addition, for a check dam, except for most of the key dams and almost all of the small and middle dams, there is only one discharge structure. Therefore, a perforated riser principal spillway often undertakes not only the function of detaining flow and retaining soil, but also draining flood water and ensuring the safety function of the dam. If flood discharge is in excess of the design discharge, then the water surface will probably be above the top of the riser, and then the riser will be regarded as the overflow pipe [26,27]. In addition, with the progression of sediment deposition behind a check dam, the orifices on the riser will be gradually buried by the trapped sediment, and the top of the riser will become the only intake; then, the riser would be regarded as the overflow pipe. However, this abnormal working condition of a perforated riser principal spillway has scarcely been studied. Based on this background, there is a need to understand the discharge capacity of this discharge structure under both normal and abnormal working conditions for the safe operation of check dams and the prediction of flood damage.

At present, there are some deficiencies in the simulations of rainfall-runoff processes in a catchment with a check-dam system equipped with a perforated riser principal spillway. On the one hand, many hydrological and hydrodynamic models cannot efficiently describe the drainage process of a perforated riser principal spillway; on the other hand, studies on the applicability and accuracy of formulas for the drainage process of a perforated riser principal spillway under both normal and abnormal working conditions need to be carried out. The main objective of this study was to improve the simulation accuracy of the rainfall-runoff process in a catchment with a check-dam system equipped with a perforated riser principal spillway. The specific objectives of this study were to (1) study the applicability and accuracy of the formula for the drainage process of a perforated riser principal spillway based on the observational experiment and propose appropriate formulas for the calculation of the discharge capacity of a perforated riser principal spillway under both normal and abnormal working conditions and (2) propose an efficient simulation scheme for the rainfall-runoff process in a catchment with a check-dam system equipped with a perforated riser principal spillway.

2. Study Site and Data

2.1. Study Area

The Wangmaogou (WMG) catchment (110°20′26″–110°22′46″ E, 37°34′13″–37°36′03″ N), located in Suide County, in the hilly and gully area of the Loess Plateau, China, was chosen for this study (Figure 1a). This catchment has an area of 5.97 km^2 with a main channel length of 3.75 km and an altitude ranging from 934.55 to 1187.75 m [28]. Loess soil is the most widely distributed soil in the studied catchment, with the characteristics of developed vertical joints, uniform particles, low clay content, and weak cementation between soil particles [29]. The average annual evaporation is 1519 mm, while the average yearly precipitation is 475.10 mm. Although precipitation varies yearly, it is distributed unevenly throughout the year. The rainfall from July to September accounts for 65% of the annual rainfall. Here, check dams are used as a key part of the management strategy to conserve soil and water. There are 23 check dams in the WMG catchment at present, and 16 of them can run normally with residual storage to trap sediments, and these 16 dams encompass 2 key check dams, 6 middle check dams and 8 small check dams, as shown in Figure 1b. Details of the check dam system are shown in Table 1.

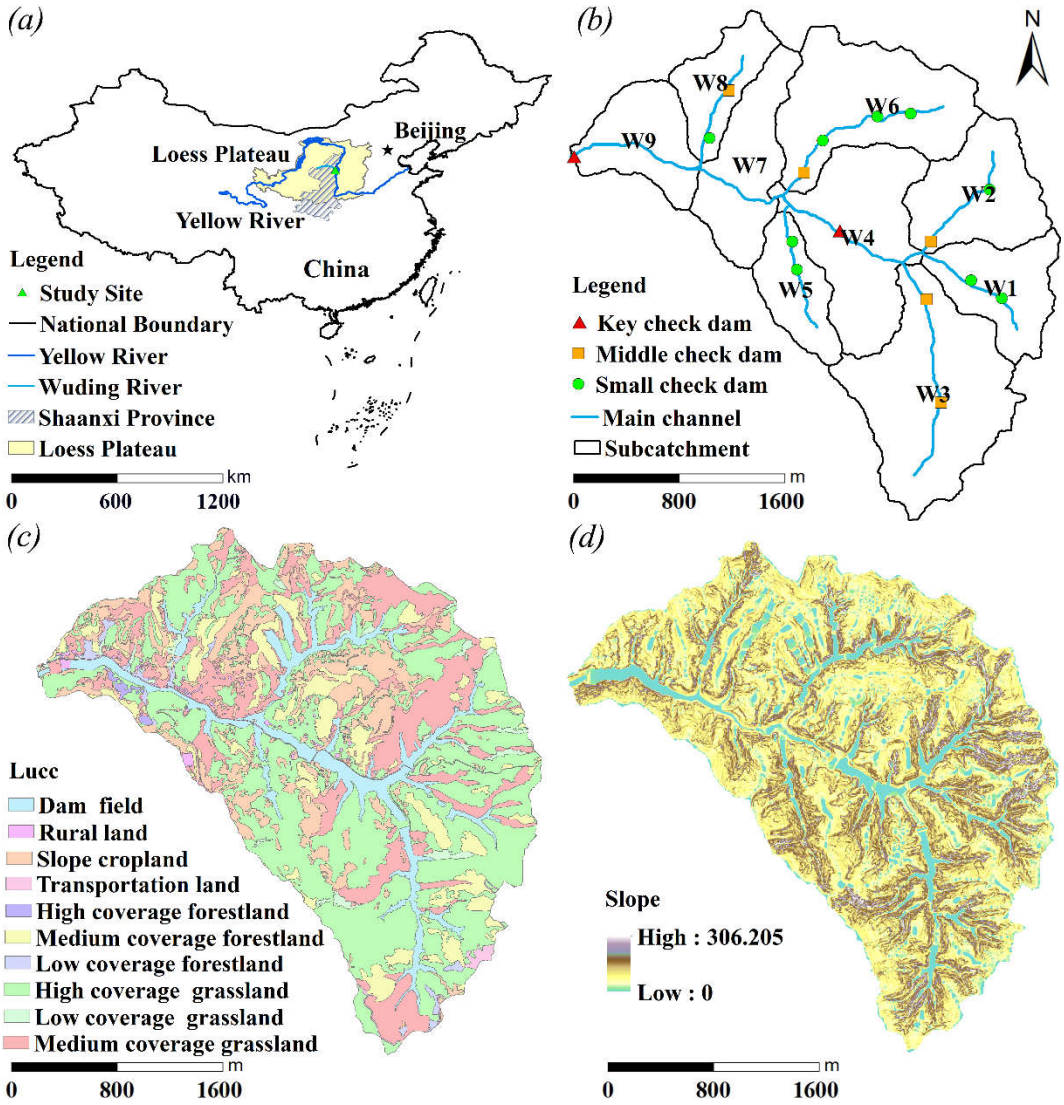

Figure 1. (**a**) Location of the study area, (**b**) check-dam distribution, (**c**) land use, and (**d**) slope.

Table 1. Basic characteristics of check dams in the WMG check dam system.

No	Name	Subcatchment	Type	Height (m)	Storage Capacity (10^4 m^3)	Residual Storage Capacity (10^4 m^3)	Drainage Structure
1	Wangtagou 2#	W1	Small	8	2.44	2.14	
2	Wangtagou 1#	W1	Small	3.6	5.11	3.11	
3	Sidizui 2#	W2	Small	20.8	15.8	5.87	
4	Sidizui 1#	W2	Middle	14.1	5.07	0.19	Perforated riser principal spillway
5	Guandigou 4#	W3	Middle	12.6	13.6	7.1	Intake pipe on the slope
6	Guandigou 1#	W3	Middle	19.5	15.03	2.53	Perforated riser principal spillway
7	Wangmaogou 2#	W4	Key	27.8	79.3	26.6	Perforated riser principal spillway
8	Kanghegou 3#	W5	Small	12.3	8.34	5.84	
9	Kanghegou 2#	W5	Small	18.2	11.5	7	Perforated riser principal spillway
10	Nianyangou 4#	W6	Small	9.4	2.4	0.3	
11	Nianyangou 3#	W6	Small	12.6	5.92	1.2	
12	Nianyangou 2#	W6	Middle	9.4	4.2	0.2	Intake pipe on the slope
13	Nianyangou 1#	W6	Middle	15.4	12.8	4.6	Perforated riser principal spillway
14	Huangbaigou 2#	W8	Small	12.1	10.3	2.3	
15	Huangbaigou 1#	W8	Middle	13.9	7.65	6.25	Perforated riser principal spillway
16	Wangmaogou 1#	W9	Key	12.7	69.83	10.63	Spillway

2.2. Data Sources and Processing

The land use in the studied catchment was visually interpreted from Google images and was divided into ten land use types (Figure 1c). The statistics of the different land-use types are provided in Table 2. The digital elevation model (DEM) of the catchment was derived from a 1:1000 topographic map.

Table 2. Land uses in the WMG catchment.

Code	Land-Use	Area (km^2)	Proportion (%)
1	Dam field	0.50	8.67
2	Rural land	0.04	0.66
3	Slope cropland	0.89	15.38
4	Transportation land	0.05	0.86
5	High coverage forestland	0.02	0.28
6	Medium coverage forestland	0.60	10.37
7	Low coverage forestland	0.05	0.83
8	High coverage grassland	2.46	42.41
9	Medium coverage grassland	1.09	18.84
10	Low coverage grassland	0.10	1.70

The rainfall and runoff data for the studied catchment were obtained from the Suide Soil and Water Conservation Monitoring Experimental Station. The rainfall-runoff process of the rainstorm event that occurred on 26 July 2017 was selected for the simulation in this study. The rainstorm began at 00:00 on 26 July 2017 and ended at 08:30 on 26 July 2017. The rainfall lasted for 8 h and 30 min, with a total rainfall of 169.9 mm and an average rainfall intensity of 19.99 mm/h. The rainfall distribution process is shown as Figure 2.

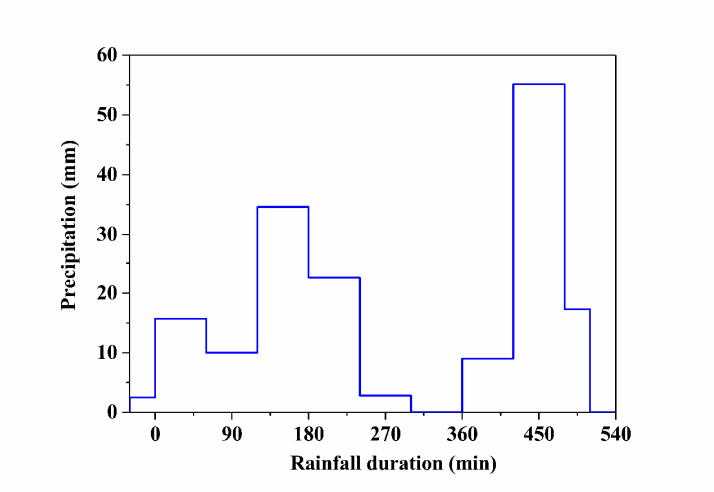

Figure 2. Rainfall distribution process of the "7.26" rainstorm event at the Wangmaogou meteorological station.

3. Method

3.1. Discharge Capacity of the Perforated Riser Principal Spillway

To clarify the discharge capacity of the spillway with a riser perforated by rectangular orifices, a laboratory experiment was carried out. The experimental arrangement (Figure 3) was a scale model of a typical perforated riser principal spillway of a check dam (Figure 4). The details of the experiment can be found in the papers by Zhang, et al. [27,30].

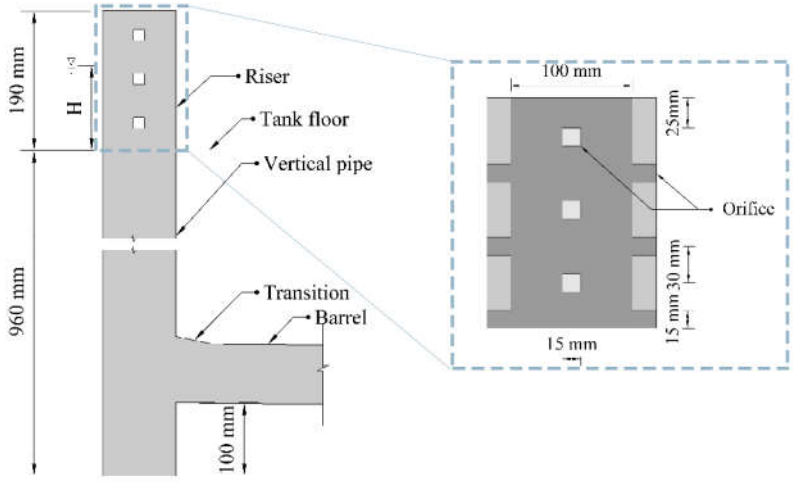

Figure 3. Profile view of the experimental perforated riser principal spillway.

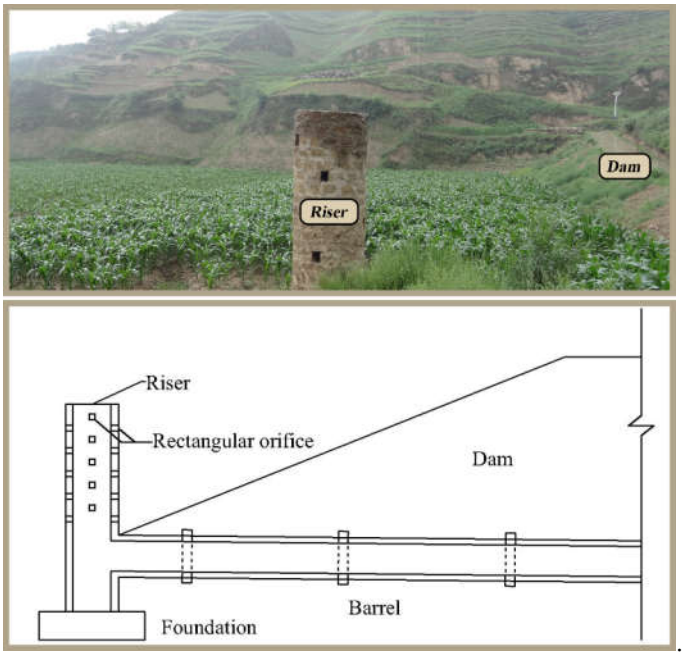

Figure 4. On-site photo and sketch of perforated riser principal spillway.

Zhang, et al. [30] studied the discharge coefficient of a perforated riser principal spillway under normal working conditions based on the experimental data and data collected from the literature, and the discharge of a single orifice on the perforated riser can be calculated by the following:

$$q = c\omega\sqrt{2gh_o} \tag{1}$$

$$c = 0.620 + 0.001\left(\frac{L}{d}\right)^{-2.737} + 0.055\left(\frac{h_o}{L}\right)^{-1.278} \tag{2}$$

where q is the discharge, m³/s; c is the discharge coefficient; ω is the area of orifices; g is the gravitational acceleration, m/s²; h_o is the head over the centerline of the orifice, m; L is the width of the rectangular orifice, m; and d is the diameter of the riser pipe.

"Technical code of key dam for soil and water conservation" [31] provides a formula for the discharge capacity of a perforated riser principal spillway under normal working conditions, which can be is calculated as the following:

$$Q = \sum_1^n \frac{1}{0.174}\omega\sqrt{h_{o_i}} \tag{3}$$

where Q is the discharge, m³/s; n is the row number of the orifices; and h_{o_i} is the head over the centerline of the orifice in the ith row.

Under abnormal working conditions of a perforated riser principal spillway, the riser can be regarded as an overflow pipe [32], and the discharge coefficient in the full flow regime C_f can be derived using the energy conservation formulas, which are the following:

$$h + z = \frac{{v_b}^2}{2g} + \zeta_e\frac{v^2}{2g} + \lambda\frac{l}{d}\frac{v^2}{2g} + \zeta_t\frac{{v_b}^2}{2g} + \lambda_b\frac{l_b}{d_b}\frac{{v_b}^2}{2g} \tag{4}$$

$$Q = \frac{\pi{d_b}^2}{4}C_f\sqrt{2g(h+z)} \tag{5}$$

$$C_f = \sqrt{\frac{1}{1 + \lambda_b \frac{l_b}{d_b} + \zeta_t + (\lambda \frac{l}{d} + \zeta_e) \frac{d_b^2}{d^2}}} \quad (6)$$

where h is the head above the top of the vertical pipe, m; z is the elevation difference between the top of the riser and the center of the barrel outlet section, m; v_b is the mean velocity in the barrel, m²/s; v is the mean velocity in the riser, m²/s; ζ_e is the entrance loss coefficient; λ is the Darcy-Weisbach friction factor; l is the length of the riser, m; ζ_t is the transition loss coefficient; l_b is the length of the barrel, m; and d_b is the inner diameter of the barrel, m.

Zhang, et al. [27] proposed an approximation for the λ of vertical pipes in the full flow regime without the Reynolds number, which is calculated as the following:

$$\frac{1}{\sqrt{\lambda}} = 0.608\left(\frac{\varepsilon}{d}\right)^{0.34} + 6.76\left(\frac{h+l}{d}\right)^{-0.34} + \left(\frac{\varepsilon}{4.03\mathrm{E}-4 \cdot d} \cdot \frac{h+l}{d}\right)^{-3} + 18.35\left(\frac{\varepsilon}{d} \cdot \frac{d}{h+l}\right)^{-0.0409} + 30.556\left(\ln\frac{h+l}{d}\right)^{-4.568} - 25.192 \quad (7)$$

where ε/d is the relative roughness of the pipe.

3.2. Modeling Approach

3.2.1. Runoff Generation

The runoff generation process was calculated by the SCS-CN model developed by the Soil Conservation Service of the United States Department of Agriculture. The SCS-CN method is based on a water balance and two fundamental hypotheses, which can be expressed as [33]

$$P = I_a + F + Q_d \quad (8)$$

$$\frac{Q_d}{P - I_a} = \frac{F}{S} \quad (9)$$

$$I_a = 0.2S \quad (10)$$

where P is the precipitation, mm; I_a is the initial abstraction, mm; F is the cumulative infiltration excluding I_a, mm; Q_d is the direct runoff, mm; and S is the potential maximum retention after the beginning of the runoff, mm.

Combining Equations (8)–(10) gives an expression for Q_d

$$Q_d = \frac{(P - 0.2S)^2}{P + 0.8S} \quad (11)$$

Equation (11) is valid for $P > I_a$, otherwise, $Q_d = 0$. The parameter S in Equation (11) is defined as

$$S = \frac{25400}{CN} - 254 \quad (12)$$

where CN depends on soil type, land use, and antecedent moisture conditions.

The Soil Conservation Service of the United States Department of Agriculture provided a tabulation for the values of CN under different conditions, in which the value of CN can be found according to the soil type and land use type. Then, the antecedent soil moisture is used to determine which level the CN belongs to; namely, drought (AMCI), general (AMCII) and wet (AMCIII). Finally, the value of CN is adjusted with the conversion formula [34].

The soil type in the studied catchment is loessal soil, which belongs to class B according to the SCS hydrologic soil groups. Before the rainstorm on 26 July 2017, the cumulative rainfall in the first 5 days was 2.2 mm, and the antecedent moisture condition was AMCI. According to the tabulation of CN values provided by the Soil Conservation Service of

the United States Department of Agriculture and the adjustment with the conversion formula, the value of CN in the studied catchment under the condition of AMCI was obtained as shown in Figure 5, and the values of CN of each subcatchment are listed in Table 3.

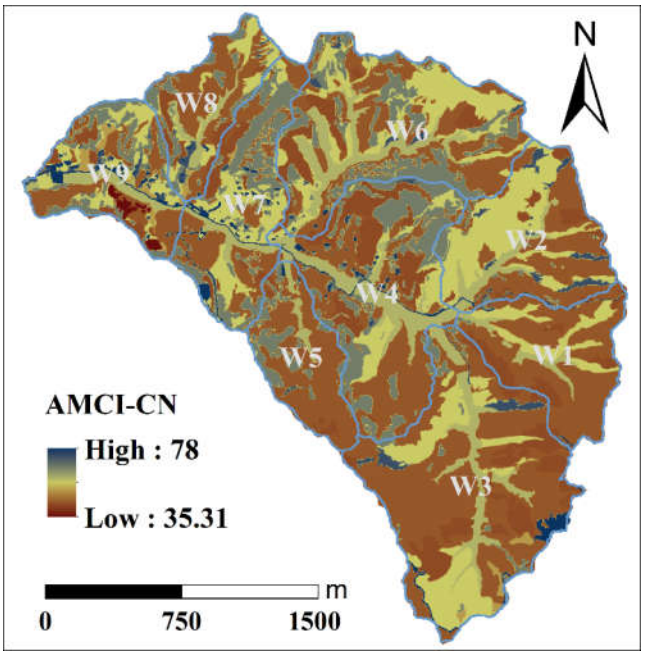

Figure 5. Values of CN in the WMG catchment under the condition of AMCI (drought).

Table 3. Values of CN and slope in the subcatchments.

Code	Subcatchment	Area (km²)	Length (km)	CN	Standard Deviation	Slope (%)	Standard Deviation (%)
1	W1	0.47	0.91	43.79	4.55	66.94	39.07
2	W2	0.60	0.94	47.37	5.96	70.74	42.87
3	W3	1.17	1.64	45.43	6.79	65.10	37.47
4	W4	0.87	1.26	48.16	7.37	56.58	33.99
5	W5	0.34	0.90	45.39	6.40	69.99	33.81
6	W6	0.93	1.43	48.44	6.26	56.48	35.88
7	W7	0.56	0.63	49.96	7.93	56.33	30.67
8	W8	0.35	0.86	46.99	6.60	61.45	34.40
9	W9	0.45	1.00	49.45	8.55	56.42	34.53

3.2.2. Direct Runoff

The surface runoff process of net rainfall in the catchment was simulated with the SCS unit hydrograph model. The SCS unit hydrograph is a dimensionless and unimodal unit hydrograph and is derived from extensive rainfall and runoff data by the Soil Conservation Service of the United States Department of Agriculture. The relationship between the peak of the unit hydrograph (U_P) and the peak time of the unit hydrograph (T_P) in the SCS unit hydrograph is [35]

$$U_P = C_c \frac{\Omega}{T_P} \quad (13)$$

where Ω is the area of a catchment, km², and C_c is the conversion constant, which is 2.08 in SI units.

The relationship between the peak time of the unit hydrograph (T_P) and the unit net rain duration (ΔT) is

$$T_P = \frac{\Delta T}{2} + T_{lag} \tag{14}$$

where T_{lag} is the lag time of a catchment, hour, namely, the difference between T_P and the peak time in the rainfall center.

T_{lag} is the only parameter that needs to be input in the SCS unit hydrograph model and can either be specified directly or may be calculated from catchment characteristics using the standard SCS formula:

$$T_{lag} = （L * 3.28 * 10^3）^{0.8} * (1000/CN - 9)^{0.7}/(1900 * Y^{0.5}) \tag{15}$$

where L is the hydraulic length of the catchment, km, and Y is the average catchment slope in percent.

3.2.3. Runoff Concentration

The runoff concentration processes in the channels were calculated with the one-dimensional Saint Venant formulas in this study. The calculations are based on several basic assumptions: the fluid is incompressible and isotropic; the slope of the riverbed is small; the flow pattern is one-dimensional flow; the hydrostatic pressure is uniform distribution; and the flow condition is subcritical flow [36].

The continuity formula and the momentum formula of the one-dimensional Saint Venant formulas are as follows:

$$\frac{\partial Q}{\partial x} + \frac{\partial A}{\partial t} = q_{in} \tag{16}$$

$$\frac{\partial Q}{\partial t} + \frac{\partial \left(\alpha \frac{Q^2}{A}\right)}{\partial x} + gA\frac{\partial h}{\partial x} + \frac{gQ|Q|}{C^2AR} = 0 \tag{17}$$

where Q is the discharge, m^3/s; x is the chainage, m; A is the cross-sectional area, m^2; t is the time, s; q_{in} is the lateral inflow, m^3/s; g is the gravitational acceleration, m/s^2; h is the water level, m; C is the Chezy coefficient, $m^{0.5}/s$; and R is the hydraulic radius, m.

The drainage process of the spillway was calculated as the broad crested weir, and the drainage process of the intake terrace on the slope is calculated with a formula suggested by the "Technical code of key dam for soil and water conservation" [31]. The drainage process of the perforated riser principal spillway was calculated with the formulas shown in Section 3.1 and was taken into the runoff concentration calculation as the depth-discharge curve.

3.3. Evaluation of Model Efficiency

In this study, the efficiency of the model was evaluated by the flood peak deviation (D), determination coefficient (R^2), and Nash efficiency coefficient (NSE), with Equations (18)–(20) [37–39]:

$$D = \frac{S_i - O_i}{O_i} \times 100 \tag{18}$$

$$R^2 = \left[\frac{\sum_{i=1}^{n}(O_i - \overline{O})(S_i - \overline{S})}{\sqrt{\sum_{i=1}^{n}(O_i - \overline{O})^2}\sqrt{\sum_{i=1}^{n}(S_i - \overline{S})^2}}\right]^2 \tag{19}$$

$$NSE = 1 - \frac{\sum_{i=1}^{n}(S_i - O_i)^2}{\sum_{i=1}^{n}(O_i - \overline{O})^2} \in (-\infty, 1] \tag{20}$$

where O_i and $\overline{O}$ are the measured and average runoff, m³/s, respectively, while S_i and $\overline{S}$ are the simulated and average runoff, m³/s, respectively.

The closer R^2 was to 1, the higher the degree of coincidence of the simulated runoff process. Moriasi, et al. [40] summarized that a simulated result could be considered perfect if its *NSE* equals 1, very good if its *NSE* falls between 0.75 and 1, good if *NSE* falls between 0.65 and 0.75, satisfactory if its *NSE* falls between 0.5 and 0.65 and unsatisfactory if the *NSE* is less than 0.5.

4. Results and Discussion

4.1. Drainage Process of the Perforated Riser Principal Spillway

To confirm the applicability of Equations (1) and (3) to the discharge process of the perforated riser principal spillway, the calculated values and the observed values are compared in Figure 6. It was shown that the discharge calculated by Equation (1) fitted the observed values better than that calculated by Equation (3), and the discharge capacity was underestimated when calculated by Equation (1). In addition, the *NSE*s of the calculated values of Equations (1) and (3) were calculated to evaluate their accuracy quantitatively. The *NSE*s of Equations (1) and (3) were 0.49 and 0.91, respectively. Therefore, Equation (1) was more appropriate than Equation (3) for describing the discharge coefficient of the perforated riser principal spillway under normal working conditions.

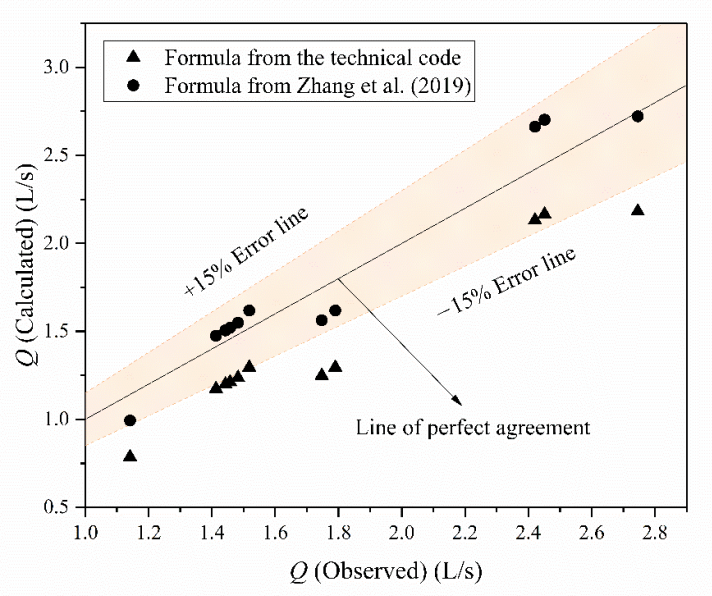

Figure 6. Comparison of the calculated discharge and the observed discharge.

The rainfall condition we selected in this study was a rainstorm event with a 100-year return period [41], which was much longer than the designed rainstorm return period of the discharge structure of a check dam. Hence, it is necessary to clarify the discharge capacity of the perforated riser principal spillway under abnormal working conditions. Under abnormal working conditions, the water surface will be above the top of the riser, and then the riser will be regarded as the overflow pipe.

The discharge capacity of a perforated riser principal spillway under abnormal working conditions was calculated by Equation (5). In the calculation, λ was calculated with Equation (7). The value of ζ_e is usually regarded as a constant [26], and the constant is valued as 0.5 in many studies [42,43]. To confirm the applicability of the value of ζ_e, the observed discharge data of Anwar [44], Banisoltan, et al. [45], Padulano, et al. [46] and Padulano, et al. [47] were cited. All of these data were obtained in the experiments for the

full flow regime of the overflow pipe, and the discharge coefficient C_f can be analytically expressed as $1/\sqrt{1+\lambda l/d+\zeta_e}$. Then, with Equation (5), the calculated value of the discharge was obtained. During the calculation, λ was calculated with Equation (7) and ζ_e was valued as 0.5. Figure 7 shows the comparison of the calculated values and the observed values, which indicated that it was appropriate to value ζ_e as 0.5. The local loss ζ_t mainly referred to the head loss that occurs in the stilling well. Guo [48] experimentally studied the energy dissipation efficiency of the stilling well in a shaft spillway, and the result showed that the value of the local loss coefficient ζ_t was approximately 3.6. This value of ζ_t was put into Equation (6), and the calculated discharge was compared with the observed values in Figure 8. The calculated discharge fit the observed values well, which indicated that the value of ζ_t was reasonable. In addition, since there is no formula recommended for the discharge capacity of a perforated riser principal spillway under abnormal working conditions in the "Technical code of key dam for soil and water conservation", we adopted a formula recommended for the intake terrace on the slope to compare with Equation (5). For this discharge structure, water was drained through the overflow intake orifice similarly, and the discharge capacity is recommended to be calculated by $(d/0.68)^2\sqrt{h}$ in the "Technical code of key dam for soil and water conservation" [31]. A comparison of the two formulas is shown in Figure 8, which indicates that the applicability of Equation (5) was better at describing the discharge capacity of the perforated riser principal spillway under abnormal working conditions.

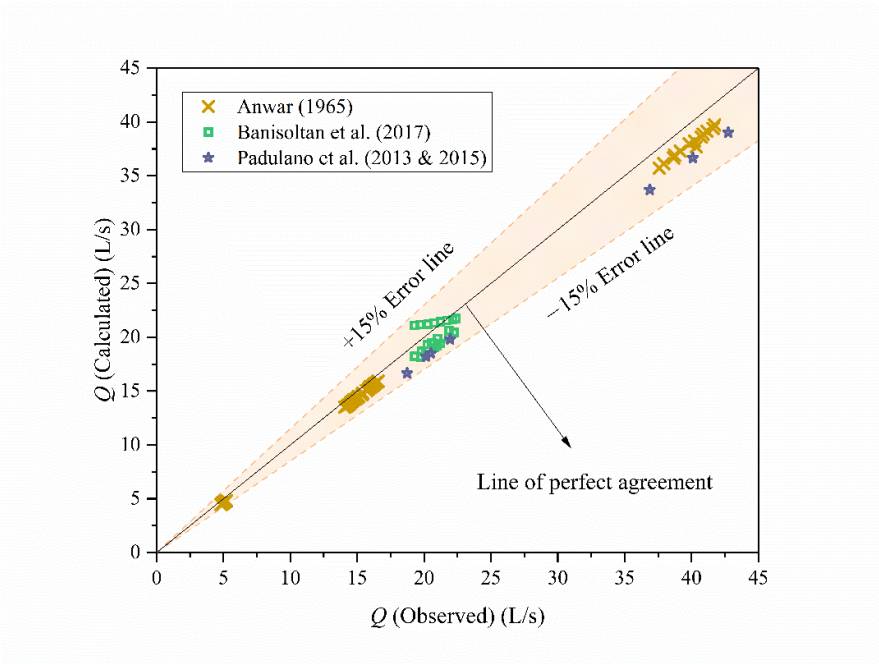

Figure 7. Comparison of the calculated discharge and the observed discharge.

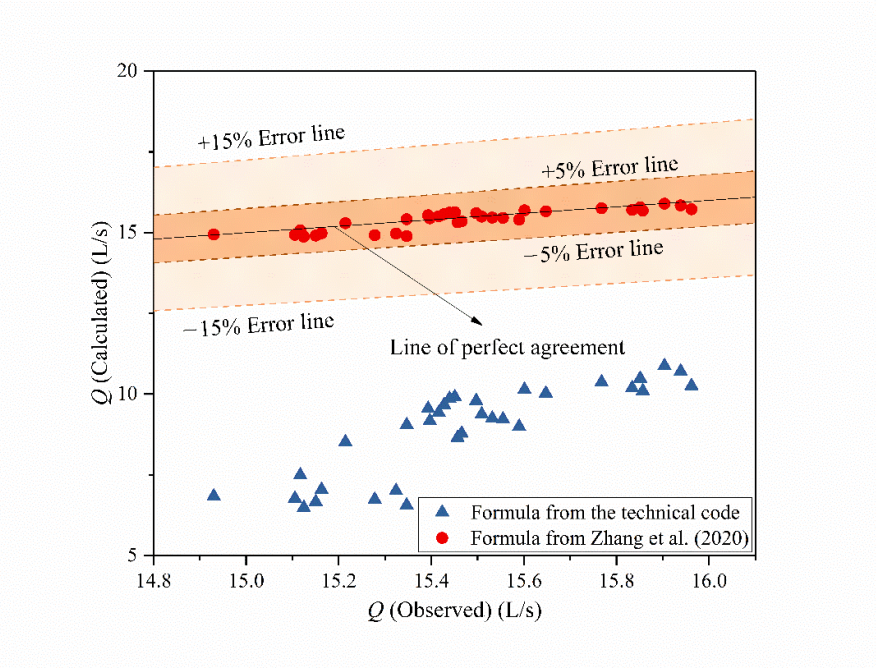

Figure 8. Comparison of the calculated discharge and the observed discharge.

4.2. Rainfall-Runoff Process in the Catchment

4.2.1. Calibration and Sensitivity Analysis of the Model Parameters

Only 2 parameters needed to be calibrated in the rainfall-runoff model used in this study; namely, the values of CN in subcatchments and the Manning coefficient. The range of the values of CN in each subcatchment was the mean value of CN in the subcatchment plus or minus the standard deviation (CN ± STD). The value range of the Manning coefficient was [0.01, 0.6], according to the related references [49]. To systematically calibrate the parameters, the CN values of each subcatchment and the Manning coefficient were set to high, medium and low and combined into 9 scenarios, as shown in Table 4. Then, the flood process caused by the rainstorm event was simulated to analyze the sensitivities of the parameters and determine a set of parameters with the highest simulation accuracy.

Table 4. Scenarios of CN and Manning coefficient combination.

Parameter	C1	C2	C3	C4	C5	C6	C7	C8	C9
CN	High	High	High	Medium	Medium	Medium	Low	Low	Low
Manning coefficient	Low	Medium	High	Low	Medium	High	Low	Medium	High

The simulated discharges in the 9 scenarios were compared with the observed data in Figure 9 and Table 5. Table 5 shows that the values of R^2 and *NSE* were largest in scenario C1, and the difference between the simulated peak discharge and the observed data was smallest. The value of *NSE* at over 0.7 in the C1 scenario indicated that the model had good simulation accuracy and could simulate the change process of the flood well. Therefore, the values of CN and the Manning coefficient in the C1 scenario were the most reasonable and can be used in the further simulation of the flood process in the catchment.

Table 5. Performance of discharge simulation over calibration processes.

Scenario	R^2	*NSE*	Peak Discharge (m^3/s)		
			Obs.	Sim.	Difference (%)
C1	0.818	0.734	24.26	20.28	16.41
C2	0.163	0.129		12.01	50.52
C3	0.021	−0.122		7.97	67.15
C4	0.761	0.719		15.21	37.31
C5	0.032	−0.119		7.66	68.44
C6	0.003	−0.257		4.66	80.79
C7	0.600	0.420		10.28	57.63
C8	0.000	−0.239		4.10	83.10
C9	0.008	−0.290		2.38	90.18

Table 5 shows that with the same CN values, the simulated result is very sensitive to the Manning coefficient, and the difference in the values of the Manning coefficient had a great influence on the *NSE* of the model. With the same value of the Manning coefficient, the influence of the values of CN on the *NSE* of the model was relatively small. Hence, the simulated result was more sensitive to the Manning coefficient than to CN.

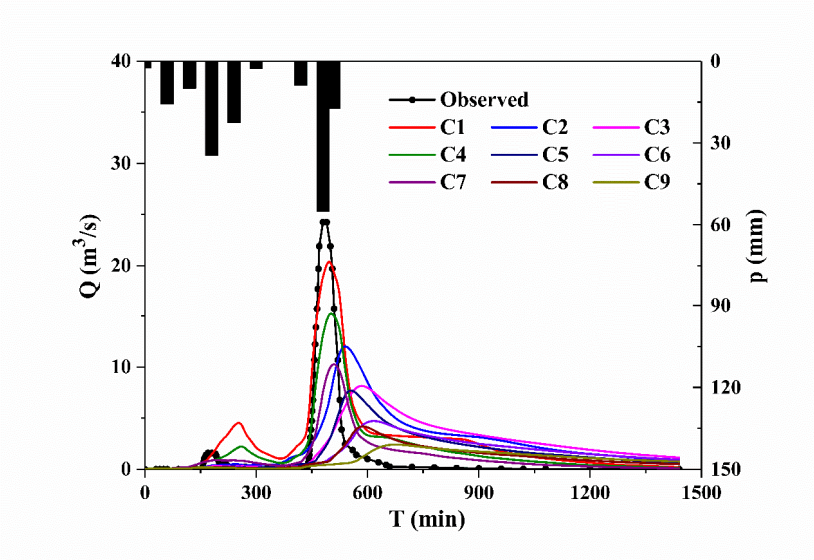

Figure 9. Comparison of the simulated and observed flood hydrographs over the calibration process.

4.2.2. Effects of Perforated Riser Principal Spillways on the Simulation Accuracy of Flood Processes

To verify the performance of the formulas for the drainage process of the perforated riser principal spillway recommended in Section 4.1 in the simulation of rainfall-runoff process, 3 scenarios—namely, the recommended formula scenario, technical code formula scenario and no drainage scenario (drainage process of the perforated riser principal spillway is ignored in the simulation)—were designed, and under these scenarios, the rainfall-runoff processes in the catchment with a check-dam system were simulated. The comparison of the simulated hydrograph and observed data in the 3 scenarios is shown in Figure 10, which indicates that all 3 simulated hydrographs describe the change process of the flood well, while the flood peak was reconstructed better in the scenario with the recommended formula scenario than in the other scenarios.

As shown in Table 6, the R^2 values of the 3 scenarios were all over 0.8, and the NSE values were all over 0.7, which indicated that the performances of the model under all 3 scenarios were good. The flood peak deviations of the 3 scenarios (the recommended formula scenario, technical code formula scenario and no drainage scenario) were 16.41%, 23.83% and 35.99%, respectively; in addition, for the recommended formula scenario, the simulation accuracy of the flood peak increased by 7.42% and 19.58% compared with accuracies of the technical code formula scenario and no drainage scenario, respectively. The R^2 and *NSE* values of the recommended formula scenario were slightly lower than those of the technical code formula scenario and no drainage scenario, which occurred mainly because the recommended formula scenario did not fit well in the small flow process of the flood retreating section. Considering that the discharge in the retreating section was far less than 1 m^3/s and the flood risk of the check-dam system is mainly caused by the large floods during its operation, it is rational to improve the simulation accuracy of the flood peak with almost unchanged model accuracy using the recommended formula scenario.

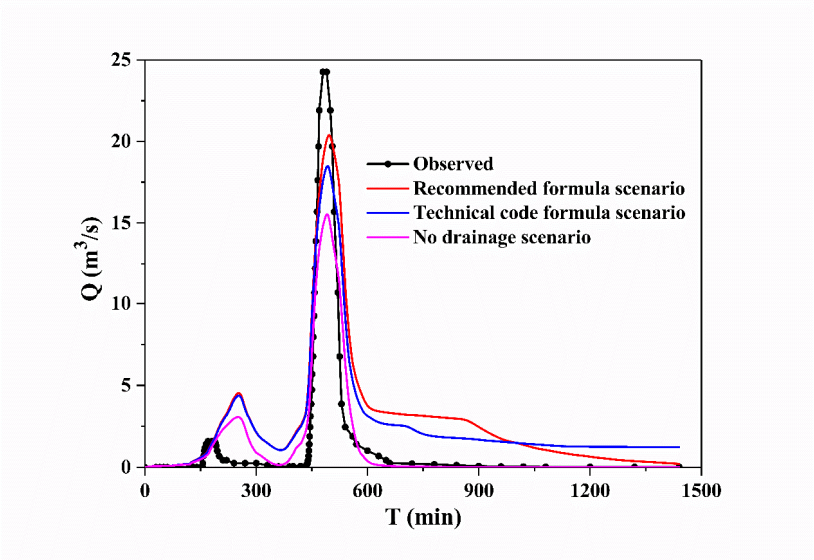

Figure 10. Comparison of the simulated hydrograph and observed data under the 3 scenarios.

Table 6. Performance of the model under the 3 scenarios.

Scenarios	R^2	*NSE*	Peak Discharge (m^3/s)		
			Obs.	Sim.	Difference (%)
Recommended formula scenario	0.82	0.73	24.26	20.28	16.41
Technical code formula scenario	0.83	0.78		18.48	23.83
No drainage scenario	0.87	0.83		15.53	35.99

5. Conclusions

This study analyzed the applicability and accuracy of the formula for the drainage process of a perforated riser principal spillway based on observational experiments, proposed appropriate formulas for the calculation of the discharge capacity of the perforated riser principal spillway under both normal and abnormal working conditions, and took the drainage process of a perforated riser principal spillway into account in the simulation of rainfall-runoff processes in a catchment with a check-dam system. The results of the sensitivity analysis showed that among the only 2 parameters that needed to be calibrated in the model used in this study, the simulation result was more sensitive to the Manning coefficient than to the CN. Parameter calibration results showed that when the CN value

was high and the Manning coefficient was low, the simulation accuracy of the model was the highest, with an *NSE* of 0.73. The recommended formulas for the drainage process of the perforated riser principal spillway can significantly improve the simulation accuracy of the flood peak, and the accuracy can be increased by 7.42% and 19.58% compared to the accuracy obtained with the technical code formula scenario and no drainage scenario. This study proposes an efficient simulation scheme for the rainfall-runoff process in a catchment with a check-dam system equipped with a perforated riser principal spillway, and provided a reference for flood warnings and the safe operation of a check-dam system.

Author Contributions: conceptualization, Z.Z. and Z.L.; methodology, Z.Z. and J.C.; formal analysis, Z.Z. and Z.X.; software, Z.Z. and S.Y.; Z.Z. wrote the manuscript and all authors contributed to improving the paper. All authors have read and agreed to the published version of the manuscript.

Funding: This work was supported by the Research Fund of the State Key Laboratory of Eco-hydraulics in Northwest Arid Region, Xi'an University of Technology (Grant No.2018KFKT-1); the Natural Science Foundation of Shaanxi Province (2017JZ013); the Leadership Talent Project of Shaanxi Province High-Level Talents Special Support Program in Science and Technology Innovation (2017); the National Natural Science Foundation of China (51679197, 41330858 and 51679193).

Institutional Review Board Statement: Not applicable.

Informed Consent Statement: Not applicable.

Data Availability Statement: All data, models, and code generated or used during the study appear in the submitted article.

Conflicts of Interest: The authors declare no conflict of interest.

Reference

1. Shi, P.; Zhang, Y.; Ren, Z.; Yu, Y.; Li, P.; Gong, J. Land-use changes and check dams reducing runoff and sediment yield on the Loess Plateau of China. *Sci. Total Environ.* **2019**, *664*, 984–994, doi:10.1016/j.scitotenv.2019.01.430.
2. Pal, D.; Galelli, S.; Tang, H.; Ran, Q. Toward improved design of check dam systems: A case study in the Loess Plateau, China. *J. Hydrol.* **2018**, *559*, 762–773, doi:10.1016/j.jhydrol.2018.02.051.
3. Abbasi, N.A.; Xu, X.; Lucas-Borja, M.E.; Dang, W.; Liu, B. The use of check dams in watershed management projects: Examples from around the world. *Sci. Total. Environ.* **2019**, *676*, 683–691, doi:10.1016/j.scitotenv.2019.04.249.
4. Xu, X.; Zhang, H.; Zhang, O. Development of check-dam systems in gullies on the Loess Plateau, China. *Environ. Sci. Policy* **2004**, *7*, 79–86, doi:10.1016/j.envsci.2003.12.002.
5. Guyassa, E.; Frankl, A.; Zenebe, A.; Poesen, J.; Nyssen, J. Effects of check dams on runoff characteristics along gully reaches, the case of Northern Ethiopia. *J. Hydrol.* **2017**, *545*, 299–309, doi:10.1016/j.jhydrol.2016.12.019.
6. Boix-Fayos, C.; Barberá, G.G.; López-Bermúdez, F.; Castillo, V.M. Effects of check dams, reforestation and land-use changes on river channel morphology: Case study of the Rogativa catchment (Murcia, Spain). *Geomorphology* **2007**, *91*, 103–123, doi:10.1016/j.geomorph.2007.02.003.
7. Castillo, V.M.; Mosch, W.M.; García, C.C.; Barberá, G.G.; Cano, J.A.N.; López-Bermúdez, F. Effectiveness and geomorphological impacts of check dams for soil erosion control in a semiarid Mediterranean catchment: El Cárcavo (Murcia, Spain). *Catena* **2007**, *70*, 416–427, doi:10.1016/j.catena.2006.11.009.
8. Hassanli, A.M.; Nameghi, A.E.; Beecham, S. Evaluation of the effect of porous check dam location on fine sediment retention (a case study). *Environ. Monit. Assess* **2009**, *152*, 319–326, doi:10.1007/s10661-008-0318-2.
9. Bombino, G.; Gurnell, A.M.; Tamburino, V.; Zema, D.A.; Zimbone, S.M. Adjustments in channel form, sediment calibre and vegetation around check-dams in the headwater reaches of mountain torrents, Calabria, Italy. *Earth Surf. Process. Landf.* **2009**, *34*, 1011–1021, doi:10.1002/esp.1791.
10. Lucas-Borja, M.E.; Zema, D.A.; Hinojosa Guzman, M.D.; Yang, Y.; Hernández, A.C.; Xiangzhou, X.; Carrà, B.G.; Nichols, M.; Cerdá, A. Exploring the influence of vegetation cover, sediment storage capacity and channel dimensions on stone check dam conditions and effectiveness in a large regulated river in México. *Ecol. Eng.* **2018**, *122*, 39–47, doi:10.1016/j.ecoleng.2018.07.025.
11. Conesa-García, C.; García-Lorenzo, R. Effectiveness of check dams in the control of general transitory bed scouring in semiarid catchment areas (South-East Spain). *Water Environ. J.* **2009**, *23*, 1–14, doi:10.1111/j.1747-6593.2007.00099.x.
12. Gao, G.; Ma, Y.; Fu, B. Multi-temporal scale changes of streamflow and sediment load in a loess hilly watershed of China. *Hydrol. Process.* **2016**, *30*, 365–382, doi:10.1002/hyp.10585.
13. Norman, L.M.; Brinkerhoff, F.; Gwilliam, E.; Guertin, D.P.; Callegary, J.; Goodrich, D.C.; Nagler, P.L.; Gray, F. Hydrologic Response of Streams Restored with Check Dams in the Chiricahua Mountains, Arizona. *River Res. Appl.* **2015**, *32*, 519–527, doi:10.1002/rra.2895.

14. Yuan, S.; Li, Z.; Li, P.; Xu, G.; Gao, H.; Xiao, L.; Wang, F.; Wang, T. Influence of Check Dams on Flood and Erosion Dynamic Processes of a Small Watershed in the Loss Plateau. *Water* **2019**, *11*, 834, doi:10.3390/w11040834.
15. Li, E.; Mu, X.; Zhao, G.; Gao, P.; Sun, W. Effects of check dams on runoff and sediment load in a semi-arid river basin of the Yellow River. *Stoch. Environ. Res. Risk Assess.* **2016**, *31*, 1791–1803, doi:10.1007/s00477-016-1333-4.
16. Xu, Y.D.; Fu, B.J.; He, C.S. Assessing the hydrological effect of the check dams in the Loess Plateau, China, by model simulations. *Hydrol. Earth Syst. Sci.* **2013**, *17*, 2185–2193, doi:10.5194/hess-17-2185-2013.
17. Kim, N.W.; Lee, J.E.; Kim, J.T. Assessment of Flow Regulation Effects by Dams in the Han River, Korea, on the Downstream Flow Regimes Using SWAT. *J. Water Resour. Plan. Manag.* **2012**, *138*, 24–35, doi:10.1061/(asce)wr.1943-5452.0000148.
18. Tang, H.; Ran, Q.; Gao, J. Physics-Based Simulation of Hydrologic Response and Sediment Transport in a Hilly-Gully Catchment with a Check Dam System on the Loess Plateau, China. *Water* **2019**, *11*, 1161, doi:10.3390/w11061161.
19. Wang, T.; Hou, J.; Li, P.; Zhao, J.; Li, Z.; Matta, E.; Ma, L.; Hinkelmann, R. Quantitative assessment of check dam system impacts on catchment flood characteristics—A case in hilly and gully area of the Loess Plateau, China. *Nat. Hazards* **2021**, *105*, 3059–3077, doi:10.1007/s11069-020-04441-7.
20. Fennessey, L.A.J.; Jarrett, A.R. Influence of principal spillway geometry and permanent pool depth on sediment retention of sedimentation basins. *Trans. ASAE* **1997**, *40*, 53–59.
21. Phillips, R.L. Tile outlet terraces-History and development. *Trans. ASAE* **1969**, *12*, 517–0518.
22. Visser, K.K.; Steichen, J.; McEnroe, B.; Hua, J. Hydraulics of perforated terrace inlet risers. *Trans. ASAE* **1988**, *31*, 1451–1454.
23. Hua, J. *Hydraulics of Terrace Intake Risers with Orifice Plates*; Kansas State University: Manhattan, Kansas, 1987.
24. McLemore, A.J.; Tyner, J.S.; Yoder, D.C.; Buchanan, J.R. Discharge coefficients for orifices cut into round pipes. *J. Irrig. Drain. Eng.* **2013**, *139*, 947–954, doi:10.1061/(ASCE)IR.1943-4774.0000641.
25. Prohaska, P.D.; Khan, A.A.; Kaye, N.B. Investigation of Flow through Orifices in Riser Pipes. *J. Irrig. Drain. Eng.* **2010**, *136*, 340–347, doi:10.1061/(ASCE)IR.1943-4774.0000195.
26. Padulano, R.; Del Giudice, G. Vertical Drain and Overflow Pipes: Literature Review and New Experimental Data. *J. Irrig. Drain. Eng.* **2018**, *144*, 04018010, doi:10.1061/(asce)ir.1943-4774.0001311.
27. Zhang, Z.; Chai, J.; Li, Z.; Xu, Z.; Li, P. Approximations of the Darcy–Weisbach friction factor in a vertical pipe with full flow regime. *Water Supply* **2020**, *20*, 1321–1333, doi:10.2166/ws.2020.048.
28. Zhao, B.; Li, Z.; Li, P.; Xu, G.; Gao, H.; Cheng, Y.; Chang, E.; Yuan, S.; Zhang, Y.; Feng, Z. Spatial distribution of soil organic carbon and its influencing factors under the condition of ecological construction in a hilly-gully watershed of the Loess Plateau, China. *Geoderma* **2017**, *296*, 10–17, doi:10.1016/j.geoderma.2017.02.010.
29. Shi, P.; Li, Z.; Li, P.; Zhang, Y.; Li, B. Trade-offs Among Ecosystem Services After Vegetation Restoration in China's Loess Plateau. *Nat. Resour. Res.* **2021**, *30*, 2703–2713, doi:10.1007/s11053-021-09841-5.
30. Zhang, Z.; Chai, J.; Li, Z.; Xu, Z.; Li, P. Discharge Coefficient of a Spillway with a Riser Perforated by Rectangular Orifices. *J. Irrig. Drain. Eng.* **2019**, *145*, 06019008, doi:10.1061/(asce)ir.1943-4774.0001425.
31. *Technical Code of Key Dam for Soil and Water Conservation;* SL289-2003; The Ministry of Water Resources of the People's Republic of China: Beijing, China, 2003. (In Chinese)
32. Kalinske, A.A. *Hydraulics of Vertical Drain and Overflow Pipes*; Iowa Institute of Hydraulics Research: Iowa City, IA, USA, 1940.
33. Verma, S.; Singh, P.K.; Mishra, S.K.; Singh, V.P.; Singh, V.; Singh, A. Activation soil moisture accounting (ASMA) for runoff estimation using soil conservation service curve number (SCS-CN) method. *J. Hydrol.* **2020**, *589*, 125114, doi:10.1016/j.jhydrol.2020.125114.
34. Mockus, V. Hydrology. In *National Engineering Handbook*; Design Hydrographs; US Soil Conservation Service: Washington, DC, USA, 1965; Volume 4.
35. Bedient, P.B.; Huber, W.C.; Vieux, B.E. *Hydrology and Floodplain Analysis*; Library of Congress Cataloging: Hudson Street, NY, USA, 2008.
36. MIKE by DHI. *MIKE 11 A Modelling System for Rivers and Channels Reference Manual*; DHI Water & Environ.: Horsholm, Denmark, 2014.
37. Henriksen, H.J.; Troldborg, L.; Nyegaard, P.; Sonnenborg, T.O.; Refsgaard, J.C.; Madsen, B. Methodology for construction, calibration and validation of a national hydrological model for Denmark. *J. Hydrol.* **2003**, *280*, 52–71, doi:10.1016/s0022-1694(03)00186-0.
38. Nash, J.E.; Sutcliffe, J.V. River flow forecasting through conceptual models part I-A discussion of principles. *J. Hydrol.* **1970**, *10*, 282–290, doi:10.1016/0022-1694(70)90255-6.
39. Tague, C.; McMichael, C.; Hope, A.; Choate, J.; Clark, R. Application of the Rhessys Model to a California Semiarid Shrubland Watershed1. *JAWRA J. Am. Water Resour. Assoc.* **2004**, *40*, 575–589, doi:10.1111/j.1752-1688.2004.tb04444.x.
40. Moriasi, D.N.; Arnold, J.G.; Liew, M.W.V.; Bingner, R.L.; Harmel, R.D.; Veith, T.L. Model Evaluation Guidelines for Systematic Quantification of Accuracy in Watershed Simulations. *Am. Soc. Agric. Biol. Eng.* **2007**, *50*, 885–900.
41. Bai, L.; Wang, N.; Jiao, J.; Chen, Y.; Tang, B.; Wang, H.; Chen, Y.; Yan, X.; Wang, Z. Soil erosion and sediment interception by check dams in a watershed for an extreme rainstorm on the Loess Plateau, China. *Int. J. Sediment Res.* **2020**, *35*, 408–416, doi:10.1016/j.ijsrc.2020.03.005.
42. Humphreys, B.H.W.; Sigurdsson, G.; Owen, H.J. *Model Test Results of Circular, Square, and Rectangular Forms of Drop-Inlet Entrance to Closed-Conduit Spillways*; Illinois State Water Survey: Urbana, IL, USA, 1970.
43. Potter, M.C.; Wiggert, D.C.; Ramadan, B.H. *Mechanics of Fluids*; Cengage Learning: Stamford, CT, USA, 2016.

44. Anwar, H. Coefficients of discharge for gravity flow into vertical pipes. *J. Hydraul. Res.* **1965**, *3*, 1–19.
45. Banisoltan, S.; Rajaratnam, N.; Zhu, D.Z. Experimental and Theoretical Investigation of Vertical Drains with Radial Inflow. *J. Hydraul. Eng.* **2017**, *143*, 04016103, doi:10.1061/(asce)hy.1943-7900.0001277.
46. Padulano, R.; Del Giudice, G.; Carravetta, A. Experimental Analysis of a Vertical Drop Shaft. *Water* **2013**, *5*, 1380–1392, doi:10.3390/w5031380.
47. Padulano, R.; Del Giudice, G.; Carravetta, A. Flow regimes in a vertical drop shaft with a sharp-edged intake. *J. Appl. Water Eng. Res.* **2015**, *3*, 29–34, doi:10.1080/23249676.2015.1026417.
48. Guo, L. *Experimental Study on Bodily from Optimization of the Shaft Spillway*; Xi'an University of Technology: Xi'an, China, 2007.
49. Ran, Q.; Hong, Y.; Chen, X.; Gao, J.; Ye, S. Impact of soil properties on water and sediment transport: A case study at a small catchment in the Loess Plateau. *J. Hydrol.* **2019**, *574*, 211–225, doi:10.1016/j.jhydrol.2019.04.040.